PHYSICAL REVIEW B **76**, 054504 (2007)

Critical-state analysis of orthogonal flux interactions in pinned superconductors

A. Badía-Majós[1,*] and C. López[2]
[1]*Departamento de Física de la Materia Condensada-ICMA, Universidad de Zaragoza-CSIC, María de Luna 1, E-50018 Zaragoza, Spain*
[2]*Departamento de Matemáticas, Universidad de Alcalá de Henares, E-28871 Alcalá de Henares, Spain*
(Received 27 April 2007; revised manuscript received 21 June 2007; published 6 August 2007)

We show that, based on the Bean model for vortex pinning [Rev. Mod. Phys. **36**, 31 (1964)] one can assess the relaxation of magnetic moment components in hard superconductors, induced by the oscillations of a perpendicular magnetic field. Our theory follows a recent proposal of using phenomenological two-dimensional modeling for the description of crossed field dynamics in high-T_c superconductors [Ph. Vanderbemden *et al.*, Phys. Rev. B **75**, 174515 (2007)]. Long thick strips of rectangular cross section, subjected to a uniform magnetic field, perpendicular to the strip axis are considered. One of the components of the applied field, H_x, oscillates with a given amplitude, while the other one, H_y, remains constant. By solving a variational statement of Bean's model, we obtain stationary regimes with either saturation of the magnetization component M_y to metastable configurations or complete decay to the thermodynamic equilibrium. As a common feature, a steplike dependence in the time relaxation is predicted for both cases. The theory may be applied to long bars of arbitrary and nonhomogeneous cross section.

DOI: 10.1103/PhysRevB.76.054504 PACS number(s): 74.25.Sv, 74.25.Ha, 41.20.Gz, 02.30.Xx

I. INTRODUCTION

A somewhat surprising fact about the magnetic moment relaxation in superconductors was emphasized by Brandt and Mikitik.[1] Under certain circumstances, relaxation phenomena can be predicted within the critical-state theory,[2] completely disregarding the influence of thermally activated flux creep. The surprise comes from the consideration of the widely used one-dimensional geometries (infinite slabs and cylinders in parallel fields). In such cases, shielding current densities never lead to relaxation whatever the time dependence of the applied magnetic field is. They only switch between the values $\pm J_c$. As a consequence, trapped current loops may not be removed (but just redistributed) unless the sample is heated up.

The central idea in Ref. 1 is that taking advantage of finite size effects, one can reconcile the criticality condition $J = \pm J_c$ with the relaxation of magnetic moment components. In brief, having a higher-dimensional system, one may transfer critical current loops between mutually perpendicular planes, and thus get rid of particular pinned flux components. A simple configuration was investigated, allowing quantitative comparison to experiments. To be specific, the authors showed that when a thin superconducting strip is placed in a transverse dc field, the application of an ac field perpendicular to the dc field leads to the decay of critical currents shielding the latter. At the same time, the current distributions evolve toward a standard critical profile related to the oscillating component. It is remarkable that, although two dimensional in nature, the thin strip model may be solved via quasi-one-dimensional analysis. Namely, thanks to the smallness of the *thickness/width* ratio, the problem may be split into two coupled one-dimensional flux pinning statements.

From the physical point of view, it is of note that, within the above theory, the actual conditions of the magnetic shaking process determine either relaxation toward the true equilibrium state of the superconductor or eventual freezing into some metastable configuration. This feature is tightly linked to the critical-state physics because it depends on the amplitude of the ac field.

As a breakthrough in the above scenario, some recent research about crossed field effects in high-T_c superconductors[3] has raised doubts about the predictions of the critical-state model in this area. In particular, the transition between the complete and incomplete relaxation regimes is questioned, pointing, in general, toward the eventual suppression of the magnetic moment. Nevertheless, the comparison between the two models and the selection of a proper theoretical background deserve further study. On the one side, the authors of Ref. 3 have performed a truly two-dimensional analysis. Their modeling is realized by studying the influence of a two-component magnetic field perpendicular to the axis of a thick rectangular strip. On the other side, the investigations were done in a flux creep framework [power law $E \propto (J/J_c)^n$] and for quite specific initial conditions.

In order to fill the gap between the available studies, in the present work, we have solved the true critical-state limit ($n \to \infty$ in the above E-J law) for two-dimensional transverse flux problems under a wide range of conditions. By using this ansatz, it will be shown that either complete or incomplete flux relaxation may be expected. We have focused on a long thick strip subjected to a magnetic field perpendicular to the axis (z axis in what follows). One of its components, H_y, is fixed, and the other one, H_x, oscillates in a zigzag fashion. Recall that the actual time dependence $H_x(t)$ is not relevant to the stationary regime, because the critical-state model does not add any time constant to the flux dynamics. The response of the system is instantaneous. Note also that the currents induced by the field always flow along the strip, and thus define a *classical* transverse problem, i.e., described by the depinning threshold condition $|J_z| \leq J_{c\perp}$. This is of mention because magnetic relaxation effects related to situations in which a current component flows parallel to the local

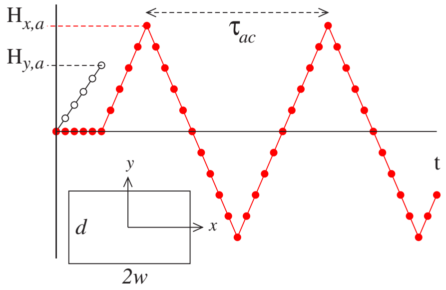

FIG. 1. (Color online) Sketch of the experiment simulated in this work. An infinite bar of cross section $2w\times d$ is subjected to the magnetic field excitation shown in the plot. H_y is initially increased to the value $H_{y,a}$ and then H_x is cycled with periodicity τ_{ac} and amplitude $H_{x,a}$.

magnetic field have also been described in the literature.[4,5] However, those studies require the incorporation of the intricate flux cutting phenomenon, through the so-called *double critical-state model*, introduced by Clem.[4] That theory includes a second parameter, $J_{c\parallel}$, related to the maximum angle between flux lines before undergoing a cutting process. Such complexity will be avoided here.

The paper is organized as follows. First, in Sec. II, we describe in detail the magnetic flux configurations under study and justify the application of a generalized Bean's model for the investigation of such phenomena. A numerical method based on the concept of mutual inductance between circuits will be introduced. In Sec. III, a set of numerical results of the actual magnetic flux dynamics in a number of crossed field configurations is presented. Based on the critical current distributions, and also related to the structure of the penetrating field lines, we show the importance of the partial penetration concept in this problem. In close analogy to the *one-dimensional* critical-state problems, increasing the applied magnetic field progressively leads to the disappearance of the flux-free region. Section. IV is devoted to the analysis of the relaxation of the magnetic moment, induced by oscillations of transverse magnetic fields. A systematic study for different amplitudes of the *polarizing* dc field as well as of the *oscillating* transverse component is presented. A relation between the decay to the true equilibrium magnetization and the disappearance of the flux-free core is established for thick samples. The generality of the above properties is shown by application of the model to samples with inhomogeneities in the cross section. Thus, in Sec. V, we illustrate the evolution of the magnetic flux structure for samples with nonhomogeneous critical current density J_c.

II. CRITICAL-STATE MODEL

The basic configuration considered in the present work is sketched in Fig. 1. A superconducting bar occupies the region defined by $|x|\leqslant w$, $|y|\leqslant d/2$, $|z|\leqslant\infty$. The external magnetic field will be applied along the x and y axes. Starting from a zero field configuration, H_y will be ramped to a final amplitude $H_{y,a}$. Then, H_x will be cycled between the values $\pm H_{x,a}$ in a linear fashion. We note that, corresponding to the hypothesis that the lower critical field of the superconductor may be neglected as compared to $H_{x,a}$ and $H_{y,a}$, the equality $\vec{B}=\mu_0\vec{H}$ will be used in what follows. In other words, the equilibrium magnetization of the sample is approximated by zero.

The starting point for the application of the critical-state theory to the above problem is our variational statement[5] within the $\{\vec{A},\vec{J}\}$ formulation.[6] Such a representation in terms of the vector potential and current density allows one to include finite size effects in a simple manner, and has been well elaborated in previous work. The equivalence to the more standard differential equation statements based on the Maxwell equations is rigorously justified in Ref. 7. Thus, the quasistationary evolution of magnetic processes in a hard superconductor may be obtained from the constrained minimization of the functional

$$\mathcal{F}\equiv\int_\Omega\int_\Omega\left[\frac{\vec{J}_{n+1}(\vec{x})\cdot\vec{J}_{n+1}(\vec{x}\,')}{|\vec{x}-\vec{x}\,'|}-2\frac{\vec{J}_{n}(\vec{x})\cdot\vec{J}_{n+1}(\vec{x}\,')}{|\vec{x}-\vec{x}\,'|}\right]+\frac{8\pi}{\mu_0}\int_\Omega(\vec{A}_{e,n+1}-\vec{A}_{e,n})\cdot\vec{J}_{n+1}(\vec{x}). \tag{1}$$

Here, $\vec{J}_n$ stands for the current density at the time layer $n\delta t$, Ω represents the superconducting region, and $\vec{A}_e$ means the externally applied vector potential. Minimization is performed iteratively in time with $\vec{J}_{n+1}(\vec{x})$ the unknown function for each step. As regards the constraints, recall that, for the present work, the minimization of $\mathcal{F}$ under the condition $\|\vec{J}\|\leqslant J_c$ will be equivalent to the flux pinning criterion $|J_\perp|\leqslant J_{c\perp}$. Indeed, from symmetry arguments it follows that $\vec{J}$ strictly flows along the bar, i.e., $\vec{J}=(0,0,J_z)$ and then $\|\vec{J}\|=|J_\perp|$.

On the technical side, an important advantage of the above mentioned problem's symmetry is the simplification of the numerical algorithm to be used for solving the variational statement. Thus, one can argue that the current density streamlines may be replaced by a collection of infinite straight wires, and the variational statement can be easily discretized to an algebraic form. The problem is transformed into the minimization of the quadratic function

$$\mathrm{F}\equiv\frac{1}{2}\sum_{i,j}I_{i,n+1}M_{ij}I_{j,n+1}-\sum_{i,j}I_{i,n}M_{ij}I_{j,n+1}+\mu_0\sum_i I_{i,n+1}(A_{e,n+1}-A_{e,n}). \tag{2}$$

Here, the set of unknowns $\{I_i\}$ represents the collection of current lines flowing across the section of the sample, and M_{ij} is their mutual inductance matrix. Minimization will be made under the set of constraints $-I_c\leqslant I_i\leqslant I_c$. The parameter I_c is the critical current for an elementary wire, related to the flux pinning current density limitation. The mutual inductance coefficients will be evaluated from the formulas (per unit length)

$$M_{ii}=\frac{\mu_0}{8\pi},$$

$$M_{ij} = \frac{\mu_0}{2\pi} \ln \frac{a^2}{(x_i - x_j)^2 + (y_i - y_j)^2}, \tag{3}$$

which can be obtained for a collection of parallel straight wires of circular cross section (radius a).[8] The simplicity of these expressions for including the inductance effects is remarkable and has been allowed by the variational statement of the problem. In fact, when dealing with infinite wires, one has to tackle with divergences caused by the unboundedness of the source. One possibility for getting rid of such difficulty is to absorb them in the form of integration constants. Thus, the vector potential created by an infinite wire carrying a current I may be written as

$$A_z = \begin{cases} (\mu_0 I/4\pi)(C - r^2/a^2), & r \leq a \\ (\mu_0 I/4\pi)[C - 1 - 2\ln(r/a)], & r > a, \end{cases} \tag{4}$$

with C the above mentioned constant. Then, if one evaluates the interaction energy $\int \vec{A}\cdot\vec{J} \equiv \Sigma_{i,j} I_i M_{ij} I_j$, that serves as the definition of M_{ij}, the constants from the different wires cancel out, and this permits the use of Eq. (3). As a first approximation, we have assumed that the vector potential created by a wire over the section of any other one may be estimated by the value at the center. This should provide a better and better approximation as the calculation grid is refined.

In summary, the calculation method is as follows. First, we compute the matrix M_{ij} for a given grid of elements, describing the problem (most of the examples presented later correspond to the rectangular case of $\ell \times m = 46 \times 92$ elements). Second, we solve the minimization of the function in Eq. (2). Recall that one has $\ell \times m$ variables ($\{I_i\}$) constrained by $\ell \times m$ conditions. This process is done iteratively in time ($n = 0, 1, 2, \ldots$) and one introduces the desired external bias, through the position dependent vector potential. In the case of a uniform field with components $(H_x, H_y, 0)$, one can use the z component $A_e = H_x y - H_y x$.

Finally, we want to mention some additional details that may be of help from the practical point of view. On the one hand the further use of symmetry considerations related to the homogeneity of the applied magnetic field is to be advised. Thus, if one considers the rectangular cross section in the inset of Fig. 1, the inversion property $I(x,y) = -I(-x, -y)$ may be recalled. Only one-half of the variables have to be accounted for, and the computation simplifies noticeably. On the other hand, an important advantage of the preferred $\{\vec{A}, \vec{J}\}$ formulation is that the physical quantities of interest are obtained by integration of the former. Then, discretization errors are smoothed. On the contrary, if one uses an $\{\vec{H}\}$ formulation, $\vec{J}$ is obtained by differentiation and this results in the magnification of errors.

III. CROSSED FIELD DYNAMICS

Below, we will present the calculated current density distributions and the corresponding magnetic field configurations induced by external excitations in the form illustrated in Fig. 1. For further analysis, we have performed calculations for a variety of values of the parameters $H_{x,a}$ and $H_{y,a}$.

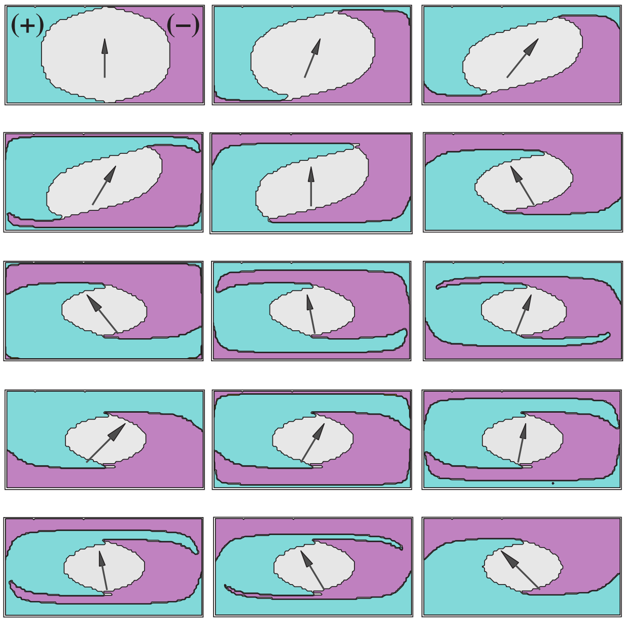

FIG. 2. (Color online) Critical current distributions within the cross section of the superconducting bar, subjected to the process in Fig. 1. The applied magnetic field vector is indicated by the central arrow. (+) indicates inward current flow, while (−) indicates outward current flow. The central core is the subcritical region $J=0$. The normalized values $h_{x,a} = h_{y,a} = 0.4$ have been used for this plot.

Both have been allowed to range well above and below the characteristic field H_p, which determines the full penetration regime for $\vec{H}$ along the x axis. Within the geometry considered in this work ($w=d$), one has[9] $H_p \simeq 0.85 w J_c/2$.

Hereafter, dimensionless units for the magnetic field will be used, in terms of H_p, i.e., $h \equiv H/H_p$.

A. Critical currents

As one expects from theoretical considerations,[5] the numerical solution of Eq. (2) produces a current density distribution with the unknowns I_i taking the values $\pm I_c, 0$. The actual structure of critical and subcritical zones within the bar's cross section strongly depends on the $\{H_x(t), H_y(t)\}$ process. Below, we describe some systematic properties that have been observed.

1. Partial penetration

In Fig. 2, we depict the critical current distributions in the initial part of the process illustrated in Fig. 1. In the upper left, one can find the typical penetration profile for a uniform external field along one of the symmetry axes of the sample (y axis). In this case, this has been achieved when the condition $h_{y,a} = 0.4$ is met. The subsequent pictures correspond to a number of intermediate steps within the first cycle for the h_x component. This has also been ramped to the amplitude $h_{x,a} = 0.4$. The actual orientation of the applied field is indicated by the central vector, that is proportional to (h_x, h_y) within each picture. Notice the similarity between the current-free cores within this study and the analytical results in Ref. 10 for thin samples in oblique fields.

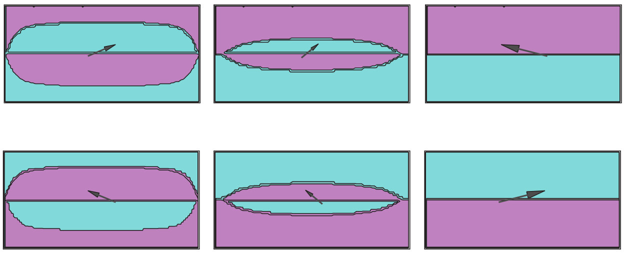

FIG. 3. (Color online) Same as Fig. 2 but using the values $h_{x,a}$=1.6 and $h_{y,a}$=0.4. Only the stationary regime after several cycles is shown.

Two facts are noticeable in the evolution of the current density penetration profiles: (i) the introduction of h_x induces upper and lower sheets of current, devoted to the shielding of the magnetic field variations, and (ii) within the chosen range of parameters, one gets a central current-free core. The core is initially distorted by the application of h_x, but rapidly acquires a stationary behavior. This property is apparent in the lower shots of Fig. 2, where we display the evolution within the first half of the second cycle in h_x. Recall that one obtains a dynamical structure for the $\pm I_c$ regions, around a stable central core with I_c=0.

2. Full penetration

As one could infer from the knowledge of one-dimensional critical-state problems, the subcritical region collapses to zero volume when the applied magnetic field reaches a certain intensity. In the two-dimensional case this is also true, but one can obtain a *full penetration* regime by combining $\{h_{x,a},h_{y,a}\}$ and the actual excitation process in a number of ways. In Fig. 3, we show the current density distributions obtained for the stationary regime in the case $h_{x,a}$=1.6, $h_{y,a}$=0.4. Recall that, together with the disappearance of the core, any trace of the initial critical state related to the application of $h_{y,a}$ is lost. The stationary critical current distribution is only related to the oscillating h_x component.

B. Magnetic flux configurations

The magnetic field profiles (applied plus induced) corresponding to the previous current density distributions are shown in Figs. 4–6. The magnetic field lines have been obtained as the contour plots of the function $A_z(x,y)$, i.e., they are given by the condition A_z=const. This is a straightforward property in the two-dimensional (2D) geometry of this work. On the other hand, Eq. (4) has been used in order to evaluate the vector potential contributed by an infinite wire of radius a and carrying a current I.

1. Partial penetration

Figure 4 displays the magnetic field structure corresponding to the transient period in which the central core is established (upper rows). Recall that the magnetic field is excluded from the current-free region (compare to Fig. 2) and also the trend of forming a stationary profile, surrounded by regions in which significant variations of the flux structure take place. Thus, in the lower rows, one can already observe that the inner core is basically unperturbed, while the applied field oscillates in between $\pm h_{x,a}$.

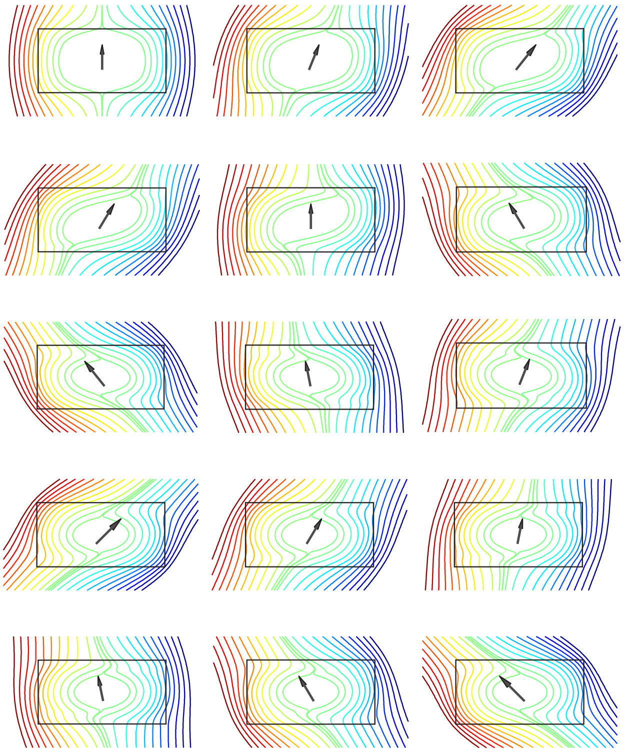

FIG. 4. (Color online) Magnetic flux lines for the process in Fig. 2. The flux-free core is defined by the two lines with the lowest magnetic field modulus within our numerical resolution.

Figure 4 has been obtained by summation over the current density profiles presented in the previous section, and thus corresponds to the crossed field amplitudes $h_{y,a}$=0.4 and $h_{x,a}$=0.4.

2. Flux-free core

In order to have a more systematic information about the partial penetration regime in 2D problems with crossed magnetic fields, we have studied the formation of the flux-free core in different conditions. Thus, Fig. 5 displays the stationary core that is obtained when one uses an oscillating field amplitude $h_{x,a}$=0.4, for initial ramps with either $h_{y,a}$=0.2 or $h_{y,a}$=0.4. The behavior for other values has been also studied, and the results (not shown for brevity) do not display significant differences.

For the sake of clarity, in the plots, we have only shown the lowest level magnetic field lines that define the core, and their evolution as h_x is cycled within the stationary regime. Notice that the boundary of the core remains unchanged, while the flux lines adapt to the applied field as one moves away from the center of the sample. The only difference between the two situations is the actual size of the core. As one can deduce from the results in the following section, this is straightforwardly related to the saturation value m_y acquired by the vertical magnetic moment.

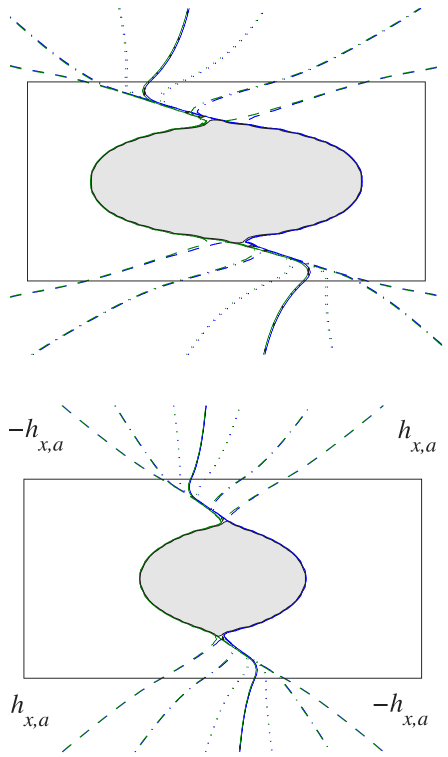

FIG. 5. (Color online) Evolution of the magnetic field lines that define the stationary flux-free core along the $\mp h_{x,a}$ cycle. The upper plot corresponds to the vertical amplitude $h_{y,a}$=0.2, while the lower one was obtained for $h_{y,a}$=0.4. Dashed, dot-dashed, dotted and, continuous styles are used for the consecutive central line pair during the cycle.

3. Full penetration

As it was shown above (Sec. III A 2), the current-free core disappears when one uses the external conditions $h_{y,a}$ =0.4 and $h_{x,a}$=1.6. Here, we show the flux line structure corresponding to the oscillations of h_x in such a range. As one can see in Fig. 6, magnetic flux has fully penetrated the sample. However, the overdamped character of flux motion in the critical state is evident in that plot. Although the flux lines close to the periphery of the sample tend to follow the external excitation, the inner regions always present a delay.

IV. MAGNETIC MOMENT RELAXATION

The connection between the magnetic field profiles obtained in the previous section, and direct experimental observations is established below. As a figure of merit, we have chosen the sample's magnetic moment (per unit length) both along the x and y axes. The definitions

$$m_x = \int_{-w}^{w} dx \int_{-d/2}^{d/2} dy[yJ_z(x,y)]$$

$$m_y = \int_{-w}^{w} dx \int_{-d/2}^{d/2} dy[xJ_z(x,y)] \tag{5}$$

have been used. These quantities are straightforwardly calculated from the current distributions $\{I_i\}$ obtained by the method in Sec. II. In practice, m_x and m_y can be measured by flux detecting coils, conveniently oriented around the sample.

Next, we discuss the influence of $h_{x,a}$ and $h_{y,a}$ on m_x and m_y, so as to provide testing criteria for our theory and also to allow comparison with the available literature on the subject.

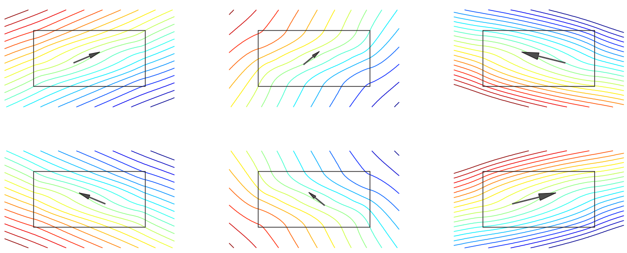

FIG. 6. (Color online) Magnetic flux lines corresponding to the full penetration profiles depicted in Fig. 3. As before, the central vector is proportional to the applied magnetic field.

A. Influence of the oscillation amplitude ($h_{x,a}$)

First, we concentrate on the effect of changing $h_{x,a}$ with $h_{y,a}$ fixed, i.e., one *polarizes* the sample by means of a given value of the vertical field and performs ac cycles of the horizontal component for different amplitudes. According to our critical-state theory, the results of such experiment would be as shown in Fig. 7. Recall that on taking $h_{y,a}$=0.4 and cycling $h_{x,a}$ between the values $\pm h_{x,a}=\pm 0.1, \pm 0.2, \pm 0.4, \pm 0.8, \pm 1.2, \pm 1.6$, m_x and m_y display a behavior which is clearly different if one probes either above or below $h_{x,a}$ =0.8.

In relation to m_x, the behavior for low amplitudes is characterized by a nonsaturated oscillation that essentially follows the applied field h_x. When plotted against this quantity, m_x reaches a stationary Bean-like loop after an initial transient in which the loop does not close. This behavior was already reported in both experimental[11] and theoretical[5] works. In the latter, in contrast to the present case, the flux cutting mechanism was considered. The response to higher amplitudes of the oscillating field ($h_{x,a}>0.8$) is characterized by a saturation of m_x, which relates to a stationary $m_x(h_x)$ loop, in the typical form of one-dimensional problems, when the full penetration regime is reached.

The properties of m_y are of special mention, since we have found less common features. Firstly, we outline the steplike behavior in the plot $m_y(t)$. Note that the descent of this quantity, induced by the oscillation of h_x, presents a series of *plateaus* that are precisely triggered by the return points in $\pm h_{x,a}$. This fact is also apparent within the $m_y(h_x)$ plot, and was mentioned before in Ref. 3, where a power law *E-J* model and the *high field* region (full penetration) were considered. Recall that here, we also obtain the steps for the low field region. Nevertheless, the early saturation of m_y makes the effect less visible in such cases.

We want to stress the high similarity of our plot $m_y(t)$ and Fig. 2. in Ref. 1. Thus, the main feature of both graphs is the

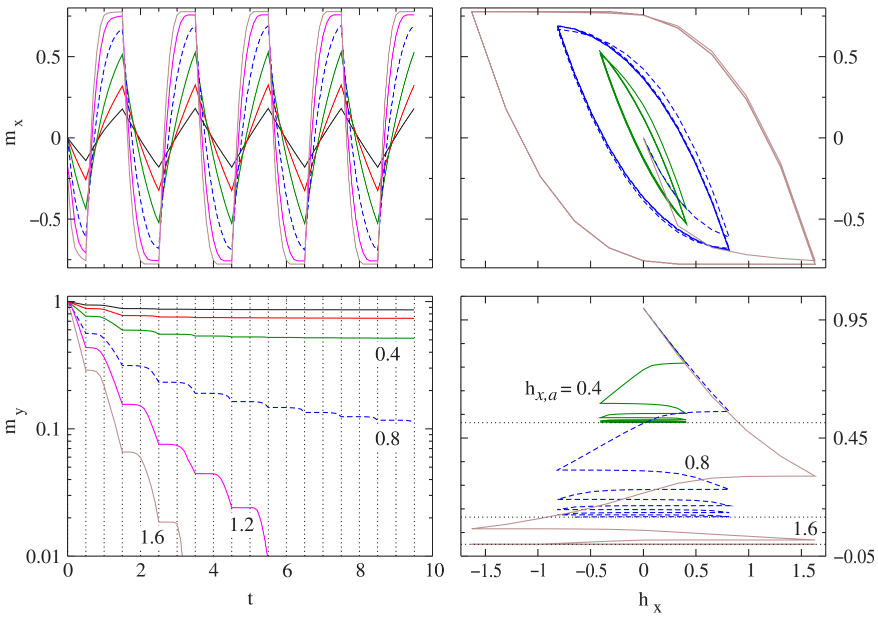

FIG. 7. (Color online) Evolution of the magnetic moment components for several excitation processes in the form sketched in Fig. 1. m_x and m_y are obtained through Eq. (5) and normalized to the values of m_y at the beginning of the ac cycle. Time (t) is given in units of $t_0 \equiv \tau_{ac} w/2d$. h_x is given in units of the penetration field H_p. The different lines (some are labeled for clarity) correspond to $h_{x,a}$=0.1, 0.2, 0.4, 0.8, 1.2, 1.6. All have been obtained for $h_{y,a}$=0.4.

separation of complete and incomplete relaxations when the value of $h_{x,a}$ approaches 1 in units of H_p. On the other side, recall that the steplike behavior in our plot would be smeared out over a time scale comparable to the one used by the authors in Ref. 1. In fact, if one takes the time unit as $t_0 \equiv \tau_{ac} w/2d$, the approximation for very thin samples used by Brandt and Mikitik leads to $t_0 \gg \tau_{ac}/2$, while in our case ($w=d$) we have $t_0=\tau_{ac}/2$.

B. Influence of the dc field amplitude ($h_{y,a}$)

Next, we analyze the relevance of the initial h_y ramp on the subsequent complete or incomplete relaxation of m_y during the h_x cycles. The main results for this study are plotted in Fig. 8. There, we show the evolution of m_y for the oscillation amplitudes $h_{x,a}$=0.2, 0.4, 0.8, 1.6 and three different values of the dc field reached in the initial stage of the process: $h_{y,a}$=0.2, 0.4, 0.8. We emphasize two aspects: (i) On the one side, the higher $h_{y,a}$, the lower value of the relaxed component $m_{y,\infty}$ when relaxation is incomplete. However, the separation between the values of $m_{y,\infty}$ first increases, and then decreases, going to zero when the complete relaxation is reached. (ii) On the other side, crossings between the values of the normalized magnetization are observed during the initial transient evolution. The importance of these crossings increases as the value of $h_{y,a}$ does.

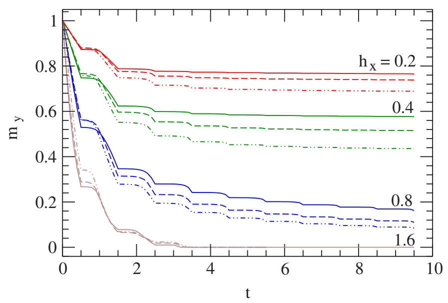

FIG. 8. (Color online) Time dependence of the normalized magnetic moment m_y at various amplitudes of the ac magnetic field $h_{x,a}$=0.2, 0.4, 0.8, 1.6. For each value of $h_{x,a}$, we compare the decay of m_y at three values of $h_{y,a}$: $h_{y,a}$=0.2 (continuous line), $h_{y,a}$=0.4 (dashed line), and $h_{y,a}$=0.8 (dot-dashed line).

V. EXTENSIONS OF THE THEORY

As an advantage of the mathematical modeling proposed in this work, one can deal with fully arbitrary 2D problems, including nonuniform magnetic fields and nonhomogeneous properties in the cross section of the sample. The $\{\vec{A},\vec{J}\}$ formulation stated in Eqs. (1) and (2) allows us to introduce irregular cross sections just by defining the positions of the appropriate elementary wires, and calculating the corresponding M_{ij} matrix.

In this section, we show the modifications introduced by a nonhomogeneous current carrying capacity. First, we calculate the evolution of the magnetic field profiles for a sample with a central hole, when subjected to the process in Fig. 1. Second, we consider the influence of having a central region with J_c noticeably above the corresponding value at the periphery of the sample.

A. Samples with holes

A sample with a hole is straightforwardly treated within the formulation in Eq. (2), just by skipping the variables related to the elementary wires within the empty region. Results are shown in Fig. 9. This plot has been obtained for the values of the applied field $h_{x,a}$=$h_{y,a}$=0.4. Several stages at the first ac cycle are shown, which already suggest the formation of a stationary regime, as in the case of Fig. 4. Nevertheless, in the present situation, the transverse field shaking process cannot induce penetration of current within the empty region. On the other side, the magnetic field lines progressively enter. Then, as a topological effect, the current-

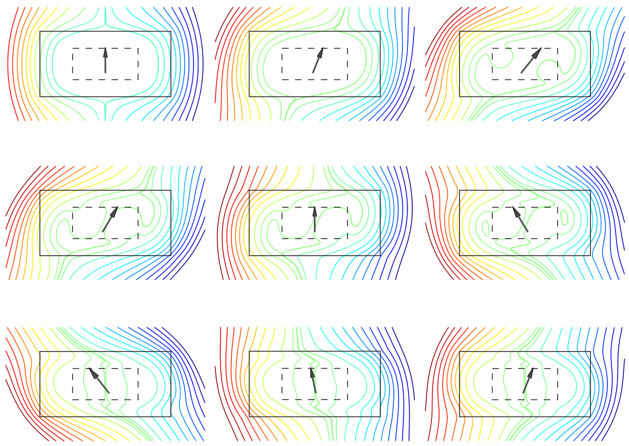

FIG. 9. (Color online) Magnetic flux lines corresponding to the excitation process in Fig. 1 for a superconducting bar with a hole (indicated by the dashed line). We show several steps at the transient process within the first cycle.

free and the flux-free regions are no longer coincident, subsequent to the contact between the penetrating flux and the hole.

Just for the sake of brevity, we do not show the stationary oscillations which follow after the last stage in Fig. 9 (one can easily guess the result). As for the case of homogeneous samples (Fig. 4), they are characterized by a frozen core and swinging flux lines in the peripheral region.

B. Nonhomogeneous critical current

Figure 10 shows the evolution of the flux penetration profiles for a sample with a higher pinning force in the central region. To be specific, we have used the ratio $J_{c,in}=5J_{c,around}$ in the simulation, i.e., the constraint for the corresponding elements is $-5I_c \leqslant I_i \leqslant 5I_c$. In dimensionless units, the applied field amplitudes are again $h_{x,a}=h_{y,a}=0.4$.

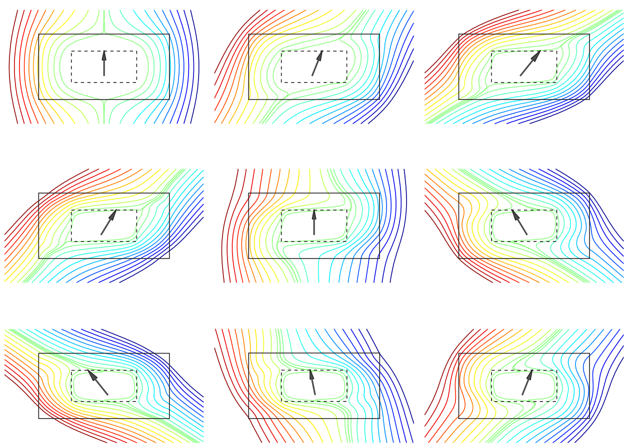

FIG. 10. (Color online) Same as Fig. 9 but for a full superconducting bar with inhomogeneous pinning properties. J_c within the dashed region is five times larger than around.

As one could expect, both flux and current penetration into the central region are hindered by the higher pinning force. Note that when the initial flux-free core is distorted by the oscillation of h_x, its boundary slips along the separation between the two regions. On the other hand, the establishment of the stationary regime basically consists of a *vertical* critical-state profile within the high J_c region and the surrounding swing of flux lines described in the previous examples.

VI. CONCLUDING REMARKS

Although the majority of theoretical and experimental studies about flux pinning in superconductors have focused on the dynamics induced by single-component applied magnetic fields, increasing interest in multicomponent situations is arising. Along this line, some recent papers[1,3–5,11,12] have considered the importance of transverse flux effects. Of particular interest is the magnetization decay induced by the oscillations of a perpendicular magnetic field. In this work, we have tried to clarify some questions about the ability of phenomenological flux pinning models for describing the experimental observations. In particular, we have addressed the debate about the existence of complete and incomplete relaxation regimes (full decay or not into the equilibrium magnetization) in terms of the actual transverse shaking process. We have shown that within the critical-state model for flux pinning, the kind of relaxation that occurs in thick samples is related to the existence of a flux-free core within the sample. Thus, under certain conditions (small enough amplitudes of the applied field components), one finds a transient regime in which the central flux-free core changes its shape until a stationary profile is reached. Afterward, the transverse field shaking produces the swing of the flux lines around the frozen core structure, and the magnetic moment becomes constant (but not zero). If the amplitude of the applied magnetic field increases enough, the flux-free core shrinks to null volume, and the stationary magnetic moment becomes zero.

The existence of incomplete and/or complete relaxation can be observed in experimental works[12] and is also predicted by the vortex-shaking model for thin samples in Ref. 1. Although there are some differences between the statement of that model and ours, the essential implications are easily reconciled. To start with, the model in Ref. 1 is a good approximation for thin strips, which are nothing but a limiting case of the 2D problem. On the other hand, it is of mention that a fundamental ingredient of Ref. 1 is the idea that flux lines *walk* toward the center of the sample ($x=0$), pivoting around the so-called *swivel points*. Switching from one swivel point to the next is done every half-cycle. In the present work, such ideas have not been recalled. Notwithstanding, we have merely used the concept of a maximum pinning force (introduced by the phenomenological parameter $J_{c\perp}$, through the restriction $|J_\perp| \leqslant J_{c\perp}$ in the variational solution of Maxwell equations). Remarkably, the evolution of flux lines in our model follows the walking pattern introduced by Brandt and Mikitik. This is shown in Fig. 11. Starting from the magnetic field profiles related to the process in Fig. 6, we have plotted a sequence of pictures, corresponding

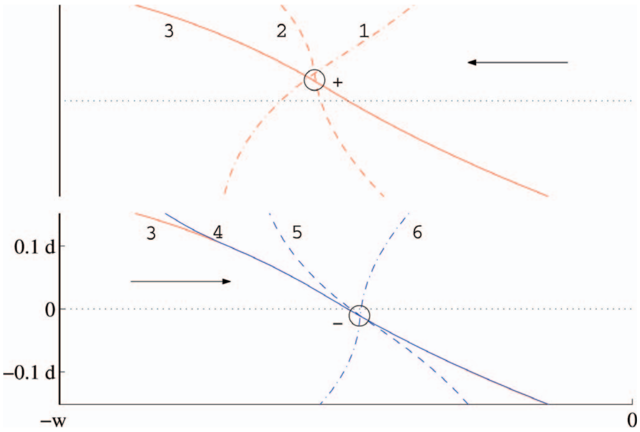

FIG. 11. (Color online) A flux line moves to the right by *pivoting* around the positions marked (+) and (−), when the ac field undergoes a cycle (sequence of numbers 1–6). The flux line has been selected from the set of profiles obtained after the conditions in Fig. 6. The picture is split into two panels for clarity.

to a specific flux line, along the first cycle. It is apparent that two swivel points are formed (labeled + and −), which establish the shift from position 1 to 6, by two rotations. The switch from the pivot + to − is clearly established by the return point $-H_{x,a}$ (step 3 to 4). We want to note that the vertical position of the swivel points has changed.

Another question to consider is the role of the aspect ratio parameter w/d. Thus, the main difference between the predicted magnetization decays, that is, the steplike structure in our Figs. 7 and 8, disappears when the physical time unit $t_0 \equiv \tau_{ac} w/2d$ is taken into account. The steps are smeared out by the time scale of the plot, and the two models coincide again.

Finally, a comparison between our proposal and the method introduced in Ref. 3 $[E \propto (J/J_c)^n]$ also seems to be of interest. In principle, the results of this paper should be obtained as the limit of the former, when higher and higher values of n are used. This would allow us to quantify the importance of flux creep effects, intrinsically included in phenomenological *E*-*J* models.

ACKNOWLEDGMENT

The authors acknowledge financial support from Spanish CICYT (Projects Nos. BMF-2003-02532 and MAT2005-06279-C03-01).

*anabadia@unizar.es

[1] E. H. Brandt and G. P. Mikitik, Phys. Rev. Lett. **89**, 027002 (2002).
[2] C. P. Bean, Rev. Mod. Phys. **36**, 31 (1964).
[3] Ph. Vanderbemden, Z. Hong, T. A. Coombs, S. Denis, M. Ausloos, J. Schwartz, I. B. Rutel, N. H. Babu, D. A. Cardwell, and A. M. Campbell, Phys. Rev. B **75**, 174515 (2007).
[4] J. R. Clem, Phys. Rev. B **26**, 2463 (1982); J. R. Clem and A. Pérez-González, *ibid.* **30**, 5041 (1984); A. Pérez-González and J. R. Clem, *ibid.* **31**, 7048 (1985); J. Appl. Phys. **58**, 4326 (1985); Phys. Rev. B **32**, 2909 (1985); J. R. Clem and A. Pérez-González, *ibid.* **33**, 1601 (1986); A. Pérez-González and J. R. Clem, *ibid.* **43**, 7792 (1991); F. Pérez-Rodríguez, A. Pérez-González, J. R. Clem, G. Gandolfini, and M. A. R. LeBlanc, *ibid.* **56**, 3473 (1997).
[5] A. Badía and C. López, Phys. Rev. Lett. **87**, 127004 (2001); Phys. Rev. B **65**, 104514 (2002).
[6] A. Badía and C. López, Appl. Phys. Lett. **86**, 202510 (2005).
[7] A. Badía, J. F. Cariñena, and C. López, J. Phys. A **39**, 14699 (2006).
[8] A. Badía, Am. J. Phys. **74**, 1136 (2006).
[9] E. H. Brandt, Phys. Rev. B **54**, 4246 (1996).
[10] G. P. Mikitik, E. H. Brandt, and M. Indenbom, Phys. Rev. B **70**, 014520 (2004).
[11] S. J. Park, J. S. Kouvel, H. B. Radousky, and J. Z. Liu, Phys. Rev. B **48**, 13998 (1993).
[12] L. M. Fisher, K. V. Il'enko, A. V. Kalinov, M. A. R. LeBlanc, F. Pérez-Rodríguez, S. E. Savel'ev, I. F. Voloshin, and V. A. Yampolskiĭ, Phys. Rev. B **61**, 15382 (2000).